Environ Monit Assess (2024) 196:1073
https://doi.org/10.1007/s10661-024-13237-2

RESEARCH

An overview of soil and plant assessment for predicting site quality and recovery strategies of one the largest tailings dam failures worldwide

Antônio Carlos Vargas Motta · Letícia de Pierri · Bernardo Lipski · Vander Freitas Melo · Maria Fernanda Dames Santos Lima · Tamires Maiara Ercole · Leonardo Pussieldi Bastos · Rodrigo Studart Corrêa

Received: 25 June 2024 / Accepted: 10 October 2024

Abstract Brazil's Fundão dam collapse is one of the world's largest disasters of tailing dam failures. Previous research has evaluated toxic metals and non-metals (Cd, Cr, Ni, Pb, As, Hg) in the same soil samples used in this study, and results have indicated that only Fe and Mn concentrations increased above the original baseline (Melo et al., 2023). Consequently, the present study's focus has shifted towards assessing and integrating changes in soil quality regarding chemical fertility and morphological, physical, and mineralogical attributes in the floodplains post-dam collapse. Soil samples from 0 to 0.2 and 0.2–0.4 m depths, and samples of *Urochloa* sp. were collected along ten transects, spanning 100 km perpendicular to the Doce River channel. This sampling strategy targeted specific landscape positions including areas affected by deposited iron tailings (DIT), soil tailing mixture (STM), and control soil (CS) devoid of iron tailing interference. Results showed no discernible alterations in Ca, Mg, K, and P concentrations in *Urochloa* sp., and the most severe negative impacts observed regarded the replacement of kaolinitic

Highlights
- Brazil's Fundão dam collapse is the world's largest disaster of tailing dam failures.
- Replacement of kaolinitic pre-disaster matrix for hematitic matrix was negative.
- Decline in physical quality: increased density and reduced macroporosity.
- The most important requirement is the augment of organic matter levels.

A. C. V. Motta · V. F. Melo (✉) · M. F. D. S. Lima
Department of Soil Science and Agricultural Engineering, Federal University of Paraná, Curitiba, PR 80035-050, Brazil
e-mail: melovander@yahoo.com.br

A. C. V. Motta
e-mail: mottaufpr@gmail.com

M. F. D. S. Lima
e-mail: mariafdames@hotmail.com

L. de Pierri
Pontifical Catholic University of Paraná (PUCPR), Curitiba, PR 80215-901, Brazil
e-mail: leticia.pierri@pucpr.br

B. Lipski · L. P. Bastos
Institute of Technology and Development (LACTEC), Curitiba, PR 80215-090, Brazil
e-mail: bernardo.lipski@lactec.com.br

L. P. Bastos
e-mail: leonardo.bastos@lactec.com.br

T. M. Ercole
Department of Soil Science, University of São Paulo (ESALQ), Piracicaba, SP 13418-260, Brazil
e-mail: tamires_98@hotmail.com

R. S. Corrêa
University of Brasília, Postgraduate in Environmental Sciences (PPGCA/FUP/UnB), Brasília, DF 73300-000, Brazil
e-mail: rscorrea@unb.br

Published online: 18 October 2024

pre-disaster matrix for hematitic matrix, reduction in organic carbon, and the prevalence of sand and silt particles. These factors collectively contributed to triggering: (i) decrease in chemical fertility and cation exchange capacity and (ii) significant decline in physical quality, evidenced by increased density and reduced total porosity and macroporosity. Addressing these adverse effects would require the augment of organic matter levels and offset the dominance of the hematitic matrix in the DIT. Furthermore, it is imperative to decompact the DIT by mechanized or plant cultivation means.

Keywords Hematite · Soil organic matter · Soil CEC · Soil density · Soil porosity

Introduction

The Fundão dam collapse in Brazil stands as a grim testament to the most extensive technological disaster among a series of global incidents involving tailing dam failures (Carmo et al., 2017; Gabriel et al., 2020). This event, which unfolded in 2015, has inflicted substantial environmental, social, and economic repercussions upon the Doce River basin, claiming the lives of 19 individuals and leading to the overflow of tailings over approximately 1614 ha. The disaster aftermath was characterized by the deposition of tailing layers with an average height of 1 m and an estimated tailing volume of 44 million cubic meters spread across the floodplains of the Doce River (Melo et al., 2023). The affected area, known as the Quadrilátero Ferrífero, houses intensive iron ore mining activities on derived metamorphic rock formation (Itabirito), which is primarily composed of quartz (70–80%), martitic hematite (20–25%), hematite (<2%), and magnetite (<0.2%) (Vasconcelos et al., 2012).

Previous investigations conducted in the region have predominantly focused on assessing the potential environmental implications associated with heavy metals and other potentially toxic elements (Coelho et al., 2020; Davila et al., 2020; Duarte et al., 2021; Hatje et al., 2017; Melo et al., 2023; Orlando et al., 2020; Queiroz et al., 2018, among several others). These studies have consistently indicated that only Fe and Mn concentrations had increased after tailing deposition onto the floodplains, remaining the other heavy metals below the original baseline concentrations. Melo et al., (2023) have concluded that the iron tailings deposited on the floodplains exhibit no present or foreseeable future potential for contamination by Ag, Ba, Cd, Co, Cr, Cu, Ni, Pb, Sb, Se, Sn, Zn, As, and Hg after investigating the same soil samples of this study (Fig. 1).

Tailings dam failures have been studied around the world: a set of 147 cases of worldwide tailings dam disasters, from which 26 located in Europe, was compiled in a database (Rico et al., 2008); for a world inventory of 18401 mine sites, the failure rate over the last 100 years is estimated to be 1.2%. This is more than two orders of magnitude higher than the failure rate of conventional water retention dams that is reported to be 0.01% (Azan and Li, 2010); global-scale impact analysis of mine tailings dam failures from 1915 to 2020 has revealed that only a few dam failure incidents have had significant impacts (Islam & Murakami, 2021); study of modeling hazard for tailings dam failures at copper mines in global supply chains has concluded that the most hazardous mines are located in Chile and Peru including some of the world's largest copper producers (Nungesser & Pauliuk, 2022); the causes and regional distribution patterns of 342 tailings dam failures globally from 1915 to 2021showed that failures occur almost every year, with an average of 4.4 accidents/year, and most tailings pond failures in Asia and Europe were related to hydroclimate, while those in South America were mainly triggered by earthquakes (Lin et al., 2022).

The present research aimed to assess changes in soil chemical fertility, physical, morphological, and mineralogical attributes in the Doce River basin's floodplains following the dam collapse to predict site quality and infer the challenges of using Technosol as the rehabilitation approach. The toxic metals and non-metals will not be evaluated here because Melo et al., (2023) have already addressed them in the same soil samples used in this study. In the present study, Technosol will be named for the deposited iron tailings, referring to soils evolved from substrates resulting from anthropogenic activities such as those exposed by mining, which demand interventions to be able to support living organisms (Rossiter, 2007).

The primary objective of this study was to conduct a comprehensive assessment and synthesis of alterations in soil quality pertaining to chemical fertility, physical, morphological, and mineralogical attributes

within the floodplains of the Doce River basin, Brazil, soon after the dam collapse. The overarching aim was to provide insights into site quality and challenges associated with the evolution of Technosols in the aftermath of such environmental disaster.

Materials and methods

Study area and soil and plant sample collection

The geographical area most profoundly impacted by the deposition of iron tailings encompasses the land extension between the Fundão dam of mining tailings and the Risoleta Neves hydroelectric power plant (Fig. 1A).

Ten cross-sections along the Gualaxo do Norte River and Carmo River channels, which are Doce River tributaries, were chosen based on their lithology, soil classes, and soil management (Melo et al., 2023). Six points were selected in each cross-section, representing different impact degrees caused by the iron tailings as follows (Fig. 1B):

i) Control soils (CS): situated at the extreme upper sides of the section, these points remained unaffected by the iron tailing deposition.
ii) Technosols: sites located on both the right and left margins of the rivers, characterized by varying levels of impact from iron tailing deposition. Specifically, two subcategories were delineated:

    a) Deposited iron tailings (DIT): represents areas where the iron tailings were directly deposited without any mixing with the original soil;
    b) Soil tailing mixture (STM): corresponds to areas where the original alluvial soil was disturbed, mixed, or covered with deposited iron tailings (Melo et al., 2023).

Composite soil samples were collected from four sub-layers spanning depths of 0–0.2 m and 0.2–0.4 m at each designated point along the cross-sections. The sampling protocol encompassed CS ($n=40$), DIT ($n=63$), and STM ($n=15$), ensuring comprehensive coverage across the affected areas. Furthermore, the study highlights the detrimental impact of the disaster on native vegetation (Fig. 1C).

Points 2 to 5 within the designated cross-sections were directly affected by the deposition of tailings. These points exhibited distinct color and purity patterns characteristic of the tailing materials, as illustrated in Fig. 2: intense red (DIT) and light yellow/red hues (STM). In section 10 (STS10), only five points were selected due to the limited areas with tailings: two red points of DIT and one yellow point of STM. Conversely, Points 1 and 6, designated as control soils (CS), consistently displayed a light yellow coloration (Fig. 2).

In the course of the study, approximately 1 kg of composite deformed samples was collected from the 0–0.2 and 0.2–0.4 m layers of the deposited iron tailings (DIT), soil tailing mixture (STM), and control soils (CS), totaling 118 composite samples. Each composite sample was formed by mixing four individual samples (Fig. 2).

Subsequent analyses encompassed the determination of consistency in the wet stage, commonly referred to as stickiness, and wet color, employing the international Munsell color standard (Munsell Soil Color Company, 1950). These assessments were conducted in all 118 composite samples. The consistency as a morphological parameter closely correlates with the quantity and quality of the clay fraction.

Only typically composite DIT samples (34 samples at the 0–0.2 m layer and 29 samples at the 0.2–0.4 m layer) were selected for the determination of organic carbon concentration, chemical fertility, and granulometry (Fig. 1B and Fig. 2) based on their morphology (only samples with intense red color and slightly sticky wet consistency) and mineralogy (samples exhibiting XRD patterns with intense peaks of hematite).

Undisturbed soil samples were also collected for physical determinations utilizing Kopecky rings measuring 2.5 cm × 6.0 cm. A single representative DIT point within each section was selected and three rings (replicates) were collected at each layer, resulting in 57 individual rings (10 sampling at 0–0.2 m and 9 sampling at 0.2–0.4 m × 3 replicates). The physical parameters were subsequently determined for each depth layer, and the reported values represent the median results obtained from the three replicates for each sampling point.

In the same cross-sections (ST1 to ST10) (Fig. 1), plants of *Urochloa* sp. (*Poaceae*) were collected during both the dry season (September 2018) and rainy

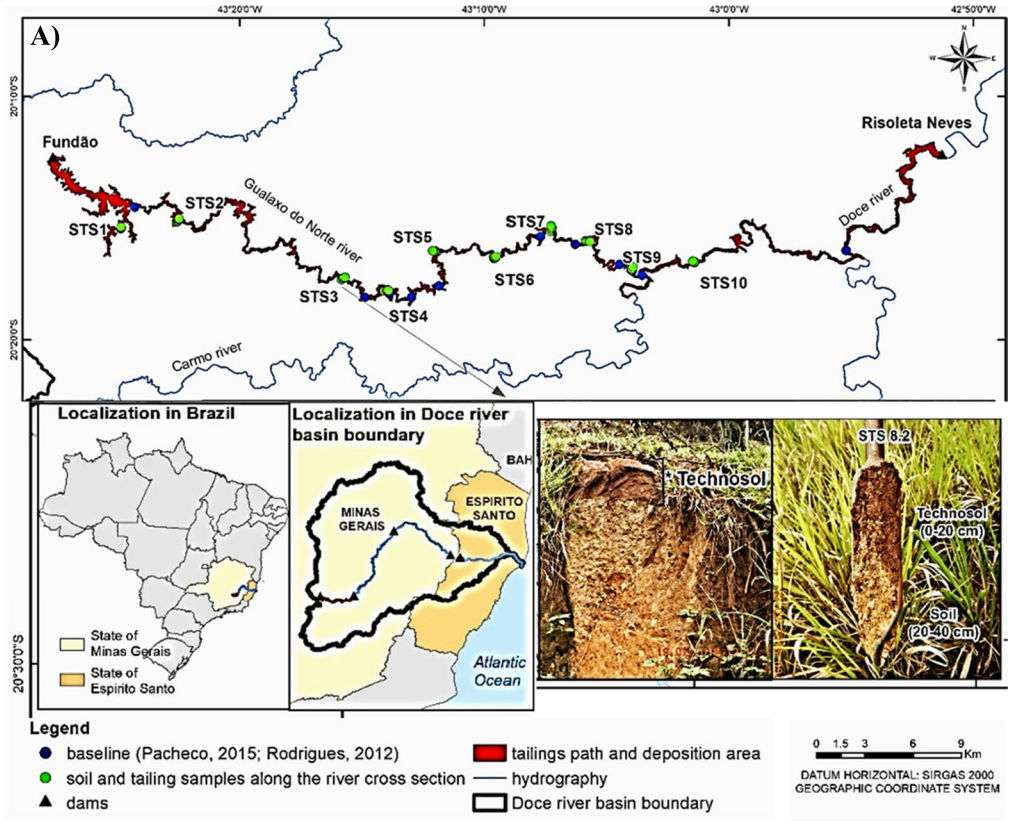
A)
43°20'0"W
43°10'0"W
43°0'0"W
42°50'0"W
20°10'0"S
20°20'0"S
20°30'0"S
Fundão
Risoleta Neves
Gualaxo do Norte river
Doce river
Carmo river
STS1
STS2
STS3
STS4
STS5
STS6
STS7
STS8
STS9
STS10
Localization in Brazil
State of Minas Gerais
State of Espirito Santo
Localization in Doce river basin boundary
BAH
MINAS GERAIS
ESPIRITO SANTO
Atlantic Ocean
Technosol
STS 8.2
Technosol (0-20 cm)
Soil (20-40 cm)
Legend
baseline (Pacheco, 2015; Rodrigues, 2012)
soil and tailing samples along the river cross section
dams
tailings path and deposition area
hydrography
Doce river basin boundary
0 1.5 3 6 9 Km
DATUM HORIZONTAL: SIRGAS 2000
GEOGRAPHIC COORDINATE SYSTEM

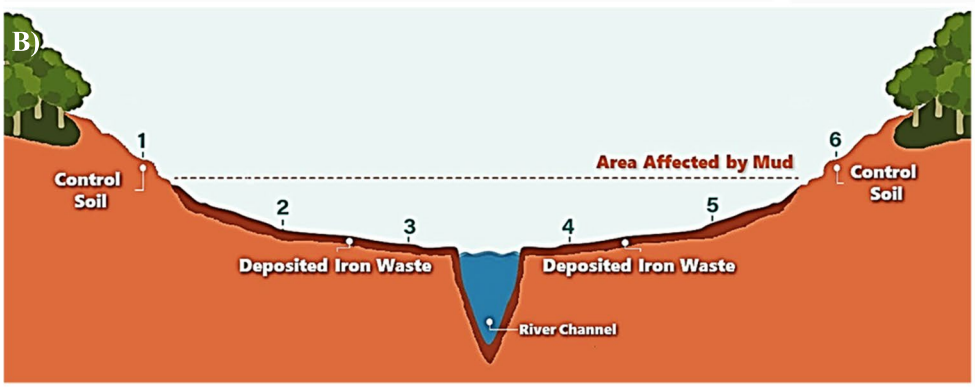
B)
Control Soil
Area Affected by Mud
Control Soil
Deposited Iron Waste
Deposited Iron Waste
River Channel
1
2
3
4
5
6


C)
1
2
3
4
5
6
Google Earth

◂**Fig. 1** **A** Partial view of Doce River basin, Fundão Dam at the studied area (floodplains between Fundão and the Risoleta Neves hydroelectric power plant), cross-sections where soil and plants were sampled (STS1–STS10), baseline points (soil samples collected pre-disaster by Rodrigues (2012) and Pacheco (2015)), and Technosol profile. **B** Schematic representation of sampling points within each cross-section (0–0.2 and 0.2–0.4 m): 1 and 6, CS; 2, 3, 4, 5, DIT and STM. **C** Example of a cross-section (aerial photo of STS1) highlighting the sampling points and negative environment impact of the disaster in native vegetation

season (February 2019). *Urochloa* sp. was selected due to its simultaneous occurrence on both control soils (CS) and in areas affected by deposited iron tailings (DIT). A total of 48 triplicate-composite shoot samples were collected to assess the nutritional status in affected (DIT) and unaffected (CS) areas using a measuring template of 0.4 × 0.4 m.

Technosol composition

Deformed samples of DIT, STM, and CS were oven-dried at 40 °C for 72 h, ground, and passed through

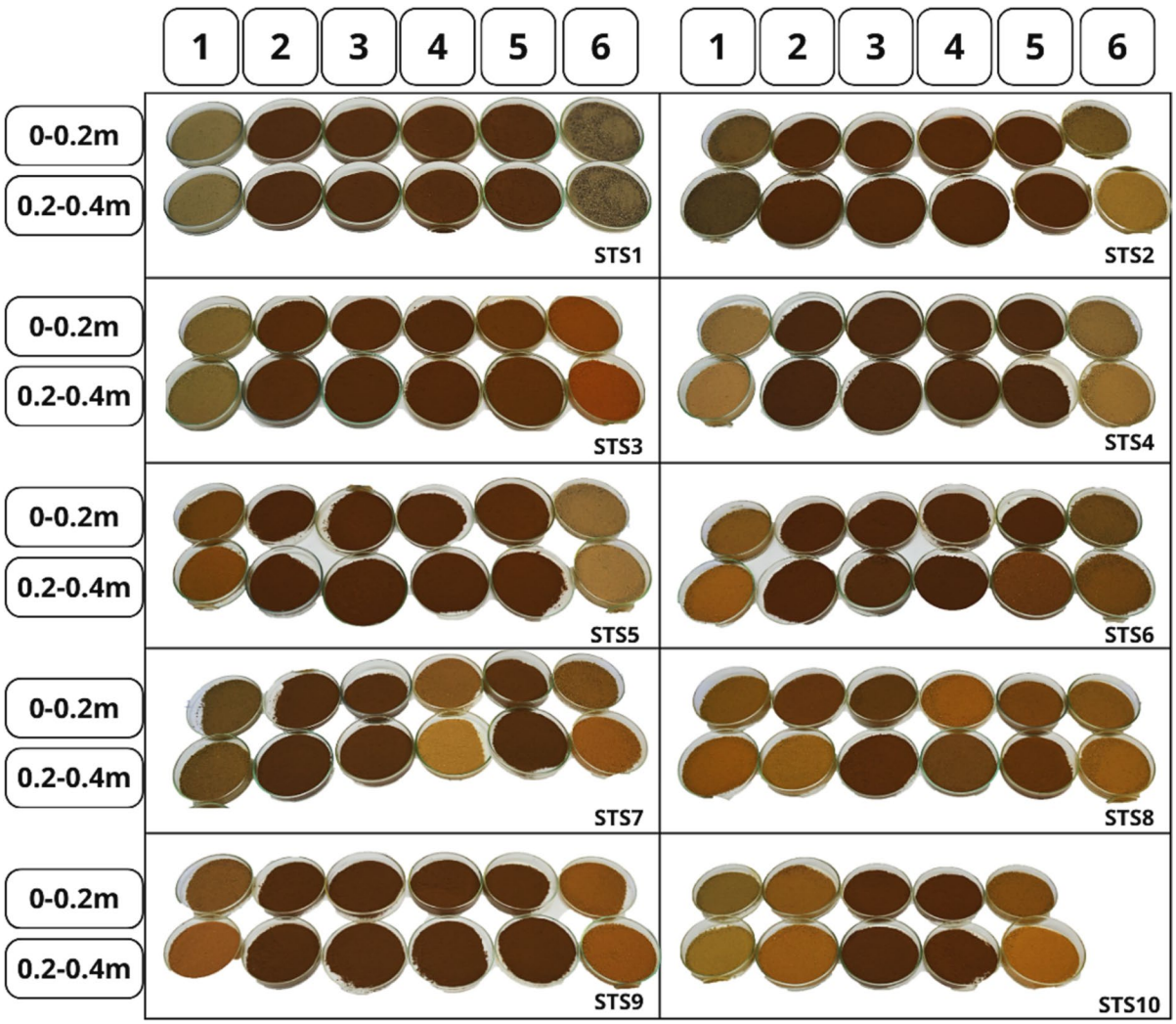

Fig. 2 Colors of dry samples of the control soil (CS: 1 and 6, right and left margins of the river, respectively) and tailings (deposited iron tailings (DIT) and soil tailing mixture (STM): 2 and 3, right; and 4 and 5, left margins of the river) in the 10 cross-sections (STS)

a 2-mm sieve (10 Mesh) to obtain the fine dry sieved fraction (FDS).

An aliquot of 0.50 g of DIT, STM, and CS (118 composite FDS samples) underwent grinding and additional sieving through a 0.2-mm sieve (70 Mesh) and subsequent X-ray diffraction (XRD) analysis. XRD patterns of the powdered samples were then obtained utilizing the Panalytical X´Pert3 apparatus, operating with a scan speed of 0.42°2θ s^{-1} and a range of 3 to 70°2θ. The diffractometer, equipped with a Ni filter, graphite monochromator, and CuKα radiation, was operated at 40 kV and 40 mA. The magnetic fraction was extracted from the sand fraction of the DIT using a hand magnet. This isolated magnetic fraction was subsequently subjected to XRD analysis within the range of 10 to 60°2θ.

Granulometry analysis was performed only for deposited iron tailings (DIT). Accordingly, a subset of 63 composite fine dry sieved (FDS) samples was subjected to examination using the pycnometer (Malvern Panalytical Zetasizer Advance) method (Embrapa, 2017). This method enables the determination of particle size distribution in four distinct size fractions: coarse sand, 0.2 to 2 mm; fine sand, 0.05 to 0.2 mm; silt, 0.002 to 0.05 mm; clay, 0.002 mm.

Additionally, the organic carbon (OC) content of the deposited iron tailings (DIT) was determined utilizing colorimetry of the Cr^{6+} ion formed through the oxidation of organic matter and subsequent reduction of dichromate (Embrapa, 2017). This analytical technique was applied exclusively to the 63 composite FDS samples from DIT.

Technosol chemical fertility

The chemical fertility parameters of the 63 composite FDS samples from DIT were determined according to Embrapa (2017): pH in H_2O, pH in KCl 1 mol L^{-1}, and pH in $CaCl_2$ 0.01 mol L^{-1}, sample:solution ratio of 1:2.5 (w/v) (Mettler Toledo, SevenExcellence pH metter S400); potential acidity (H + Al), extracted with 0.5 mol L^{-1} pH 7 calcium acetate and determined by titration; exchangeable Ca^{2+}, Mg^{2+}, and Al^{3+}, extracted with 1 mol L^{-1} KCl and determined by atomic absorption spectrophotometry (Atomic absorption spectrophotometer Varian AA240 FS); available P and exchangeable K^+ and Na^+, extracted with Mehlich-1 and determined by colorimetry (P) (Biospectro—SP22) and flame photometry (K and Na) (Digimed—NK 2000). Based on the chemical fertility data, it was calculated the sum of bases ($SB = Ca^{2+} + Mg^{2+} + K^+ + Na^+$), cation exchange capacity at soil pH ($CEC_{soil\ pH} = SB + Al$), cation exchange capacity at pH 7 [$CEC_{pH\ 7} = SB + (H + Al^{3+})$], and delta pH ($\Delta pH = pH_{KCl} - pH_{H2O}$).

Technosol physical attributes

The particle density (Dp) of disturbed samples from the deposited iron tailings (DIT) was determined utilizing the volumetric flask filled with ethyl alcohol method (Embrapa, 2017).

The other physical parameters were determined in undisturbed samples collected via Kopech ring methodology (Brady & Weil, 2002; Embrapa, 2017). It was sampled 19 points, being 10 at 0–0.2 m and 9 at 0.2–0.4 m × 3 replicate = 57 individual rings of DIT (Brady & Weil, 2002; Embrapa, 2017). Bulk density (Db—g cm^{-3}) consisted in weighing sample mass dried at 105 °C for 12 h and divide it by the ring volume; field capacity (FC) was measured in water-saturated soil samples placed in a tension table for 48 h at − 0.01 MPa; permanent wilting point (PWP) considered the same samples placed in a Richard chamber for 48 h at − 1.5 MP; total porosity (TP), microporosity (Mi), macroporosity (Ma) measurements based on water-saturated samples are subjected to a tension table at 60 cm of water column for the removal of water from Ma (diameter ≥ 0.05 mm). After removing water from Ma, samples were weighed and dried in an oven at 105 °C for 12 h for the respective determination of macro (Ma) and micropore (Mi) volumes as follows (Eq. 1):

$$TP(m^3 m^{-3}) = (Dp - Db)/Dp \quad (1)$$

$$Mi(m^3 m^{-3}) = (a - b)/c$$

where:

a	is the sample mass after applying a tension of 60 cm of water column (g)
b	is the dry sample mass at 105 °C (g)
c	is the ring volume (m^3)
Ma (m^3 m^{-3})	= total porosity – microporosity

The available water capacity (AWC) was calculated from Eq. 2:

$$AWC(mm) = (FC - PWP) \times Db \times z \times 10 \quad (2)$$

where z is the layer thickness (mm).

Plant (*Urochloa* sp.) nutritional composition

The shoot biomass of *Urochloa* sp. collected from both the deposited iron tailings (DIT, 24 composite samples) and control soils (CS, 24 composite samples) were washed with running and deionized water, dried at 60 °C in a forced-air oven until reaching constant weight, and ground to powder using a Wiley mill. Subsequently, approximately 0.3000 g of ground plant sample was transferred into Teflon tubes in the presence of 7 mL of 50% (v/v) HNO_3 and 2 mL of 30% (v/v) H_2O_2. The Teflon tubes were sealed and placed in a microwave oven MarsXpress 6, CEM for 20 min until the temperature reached 180 °C, maintained for an additional 15 min. The solution was filtered through paper, and macronutrients (Ca, Mg, K, and P) in it were analyzed by inductively coupled plasma optical emission spectroscopy (ICP-OES) (Varian 720-ES).

Data analysis

Descriptive statistics

The chemical and physical data were represented by median values and quartiles (25th and 75th) in Boxplots (software SigmaPlot 14.0®). Results were assessed for normality and variance homogeneity (Kruskal–Wallis test), using R software, version 3.5.1.

To establish a comprehensive baseline for the physical and chemical attributes of the soil in the study area, data from alluvial soils pre-dating the disaster were utilized. These data were obtained from previous studies by Rodrigues (2012) and Pacheco (2015). However, to ensure the compatibility of methodologies and create a cohesive baseline dataset, a careful analysis was conducted by Melo et al., (2023).

For physical attributes such as bulk density (Ds), particle density (Dp), total porosity (TP), microporosity (Mi), macroporosity (Ma), and available water capacity (AWC) that were not directly determined by Pacheco (2015) and/or Rodrigues (2012), additional soil profiles were selected from the Brazilian soil hydrophysical database (Hybras 1.0) (Ottoni et al., 2018). To select these hydromorphic profiles, care was taken to define soils corresponding to the same granulometric range, particle density, and organic carbon content observed in the soil profiles of the Pacheco (2015) used as baseline for the other parameters. The granulometry was directly compared with the data from Pacheco (2015).

Nutritional status of the plants

In the absence of pre-disaster (baseline) data on the nutritional state of plants, comparisons were made based on the composition of *Urochloa* sp. in different positions along the transect, specifically comparing the plant samples collected from the deposited iron tailings (DIT) versus control soils (CS). The macronutrient contents in the plant tissue were represented using median values and quartiles (25th and 75th percentiles) in the form of Boxplots, which were generated using SigmaPlot 14.0® software.

Results and discussion

Technosol morphology and composition

The analysis of sediment composition post-tailing deposition in the floodplains has revealed a significant increase in it silt content (Fig. 3), which has been consistently observed in various studies conducted along the Doce River floodplain following the dam disaster (Silva et al., 2021).

Median values for total sand (444 g kg^{-1}) and fine sand (368 g kg^{-1}) in the 0–0.2 m DIT layer were lower than the median baseline (695 and 600 g kg^{-1}, respectively). Median values of coarse sand (67 g kg^{-1}) and clay (150 g kg^{-1}) were similar to baseline values (75 and 150 g kg^{-1}, respectively). The granulometry of the Technosol was uniform throughout the depths (Fig. 3), and it indicates homogeneity in the deposition of tailings. Such texture homogeneity can be attributed to the iron ore beneficiation process, which involves stages of screening, grinding, desliming, and flotation. The grinding and screening stages of this process effectively reduce particle sizes to the silt range (Vasconcelos et al., 2012).

All ten sections have exhibited the presence of hematite (Hm) peaks and residual goethite (Gt) in their X-ray diffraction (XRD) patterns (Fig. 4). The substantial occurrence of quartz in the DIT reflects

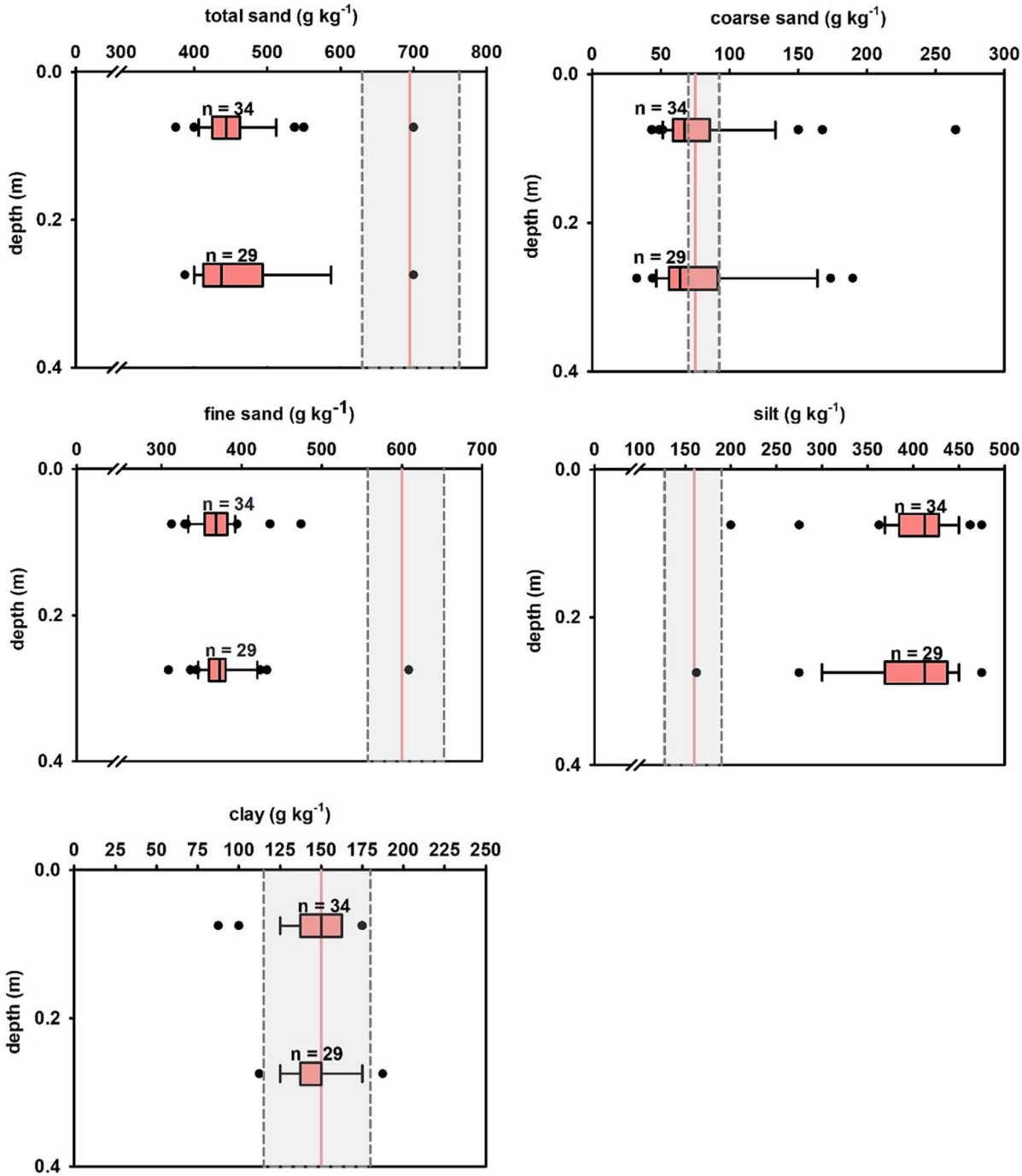

Fig. 3 Total sand, coarse sand, fine sand, silt, and clay concentrations in Technosols (deposited iron tailings (DIT)) collected across 10 cross-sections in the Doce River basin. Vertical dotted lines separated by shaded areas represent the first and third quartiles of the baseline, and the red vertical line represents the baseline median (Pacheco, 2015)

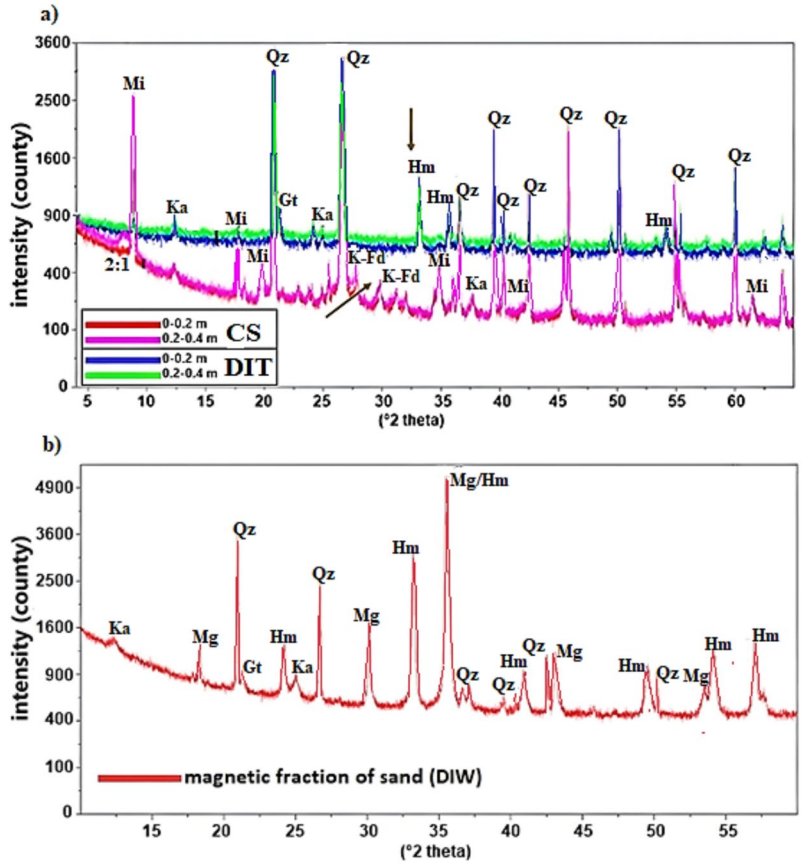

Fig. 4 X-ray diffractograms of the samples 5 (deposited iron tailings (DIT)) and 6 (control soils (CS)) of the ST4 transect (representatives of all samples), highlighting the intense peak of Hm (**a**) and magnetic in sand fraction extracted from the sample ST4-5 (**b**). 2:1, secondary 2:1 phyllosilicate mineral; Ka, kaolinite; Mi, mica; Il, illite; Gt, goethite; Hm, hematite; Mg, magnetite; Qz, quartz; K-Fd, potassium feldspar

the composition of the metamorphic rock (Itabirito) used in the iron mining process: quartz (70–80%), martitic hematite (20–25%), hematite (< 2%), and magnetite (< 0.2%) (Vasconcelos et al., 2012). The Hm in the DIT is lithogenic (primary) and mainly presents fine sand and silt sizes (Fig. 3).

The enrichment of Hm and magnetite is more noticeable in the magnetic DIT's sand fraction (Fig. 4). Geology strongly affects magnetic susceptibility (κ), mainly in basic-derived soils (Mello et al., 2020). In fluvial sediments, the κ values can be used as sediment source fingerprinting procedures (Pulley et al., 2018). The presence of quartz in the magnetic fraction (Fig. 4) can be attributed to the separation of magnet of silicate fragments from the rock (Itabirito), which drags the silicate mineral together with the magnetic Fe oxides. Other authors have also found an increase in hematite in the floodplains post-dam disaster (Orlando et al., 2020; Queiroz et al., 2018).

Iron oxides were not identified in control soils (CS) (Fig. 4), but secondary 2:1 phyllosilicate mineral and 1:1 (kaolinite) have predominated at the transect margins (samples 1 and 6, CS). This mineralogical composition is consistent with the influence of the underlying granite/gneiss bedrock, characterized by abundant occurrences of quartz, mica, and K-feldspar (Almeida et al., 2018). In contrast to the floodplain soils post-dam disaster, the floodplain soils pre-disaster (baseline) have exhibited a different mineral assemblage.., kaolinite, gibbsite, and residues of hematite (Hm) and goethite (Gt) (Pacheco, 2015; Rodrigues, 2012). However, the intensity of XRD peaks associated with hematite and goethite was relatively low in the pre-disaster samples.

The intense presence of hematite (Hm) in the XRD patterns (Fig. 4) and the prevalence of silt particles (Fig. 3) in the deposited iron tailings (DIT) delineate its morphological characteristics like intense red color (hue 7.5R and 10R) and a slightly sticky consistency (Table 1). Such a characteristic observed in the DIT can be attributed to the combination of factors such as the low activity of 1:1 clay mineral (such as kaolinite)

Table 1 Wet sample color (hue, value, and chroma) and wet consistency (stickiness) of control soils (CS), deposited iron tailings (DIT), and soil tailing mixture (STM) from representative cross-sections along the study area (10 cross-sections and a total of 118 determinations for both color and consistency). The visual aspect of the dry color can be seen in Fig. 2

Depth	Croos-section/sampling point					
	3.1	3.2	3.3	3.4	3.5	3.6
	CS	DIT	DIT	DIT	DIT	CS
0–0.2 m	10YR 7/8	10R 4/4	10R 4/3	10R 4/4	10R 5/6	2.5YR 5/6
	Sticky	Slightly sticky ligeiramente pegajoso	Slightly sticky	Slightly sticky	Slightly sticky	Sticky
		DIT	DIT	DIT	DIT	
0.2–0.4 m	10YR 5/6	10R 4/3	7.5R 4/4	10R 4/3	10R 6/6	5YR 5/6
	Sticky	Slightly sticky	Slightly sticky	Slightly sticky	Slightly sticky	Sticky
	6.1	6.2	6.3	6.4	6.5	6.6
	CS	DIT	DIT	DIT	DIT	CS
0–0.2 m	10YR 6/6	7.5R 4/3	7.5R 4/3	7.5R 4/3	7.5R 4/3	10YR 3/4
	Sticky	Slightly sticky	Slightly sticky	Slightly sticky	Slightly sticky	Sticky
		DIT	DIT	DIT	STM	
0.2–0.4 m	7.5YR 5/8	7.5R 4/3	7.5R 4/3	10R 4/3	5YR 5/6	7.5YR 6/6
	Sticky	Slightly sticky	Slightly sticky	Slightly sticky	Slightly sticky	Sticky

and the presence of iron oxides in the clay fraction, coupled with elevated levels of sand and silt particles. Distinct from the DIT, the soil tailing mixture (STM) samples have exhibited a noticeable yellowish hue, exemplified by sample 5 at a depth of 0.2–0.4 m in section 6 (hue 5YR) (Table 1). It is worth noting that the Fluvic Entisol profile characterized by Pacheco (2015) before de dam disaster (baseline) displayed a consistent yellowish hue (7.5YR) throughout the entire soil profile (from 0 to 1.8 m depth).

The organic phase of the Technosols has undergone significant negative alterations compared to soils pre-disaster, with organic carbon (OC) levels notably lower than in the baseline soils (Fig. 5).

In an integrative analysis, the deposited iron tailings (DIT) have induced multiple changes in soil characteristics, including an increase in silt content, a transition from a kaolinitic matrix to a hematitic matrix, and a reduction in organic matter content. These alterations have led to several negative consequences such as (i) hindered aeration in DIT as silt particles filled the free spaces between sand particles (Gamie & Smedt, 2017; Ramos et al., 2015) and (ii) dominance of positive charges, which reduce cation adsorption capacity and increase the leaching of cationic pollutants as an environmental vulnerability (Melo et al., 2023).

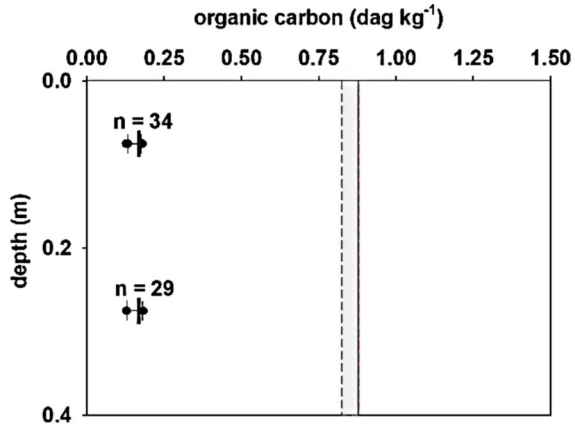

Fig. 5 Organic carbon concentration in Technosols (deposited iron tailings (DIT)) collected from 10 cross-sections in the Doce River basin. Vertical lines separated by hatched areas represent the first and third quartile limits of the baseline

Technosol physical attributes

The bulk density (Db) of the deposited iron tailings (DIT) has increased when compared with the baseline soils, and it correlated with its lower total porosity (TP) and higher particle density (Dp) (Fig. 6). The median TP values of the DIT have been lower than in the baseline soils, and such reduction in TP can be

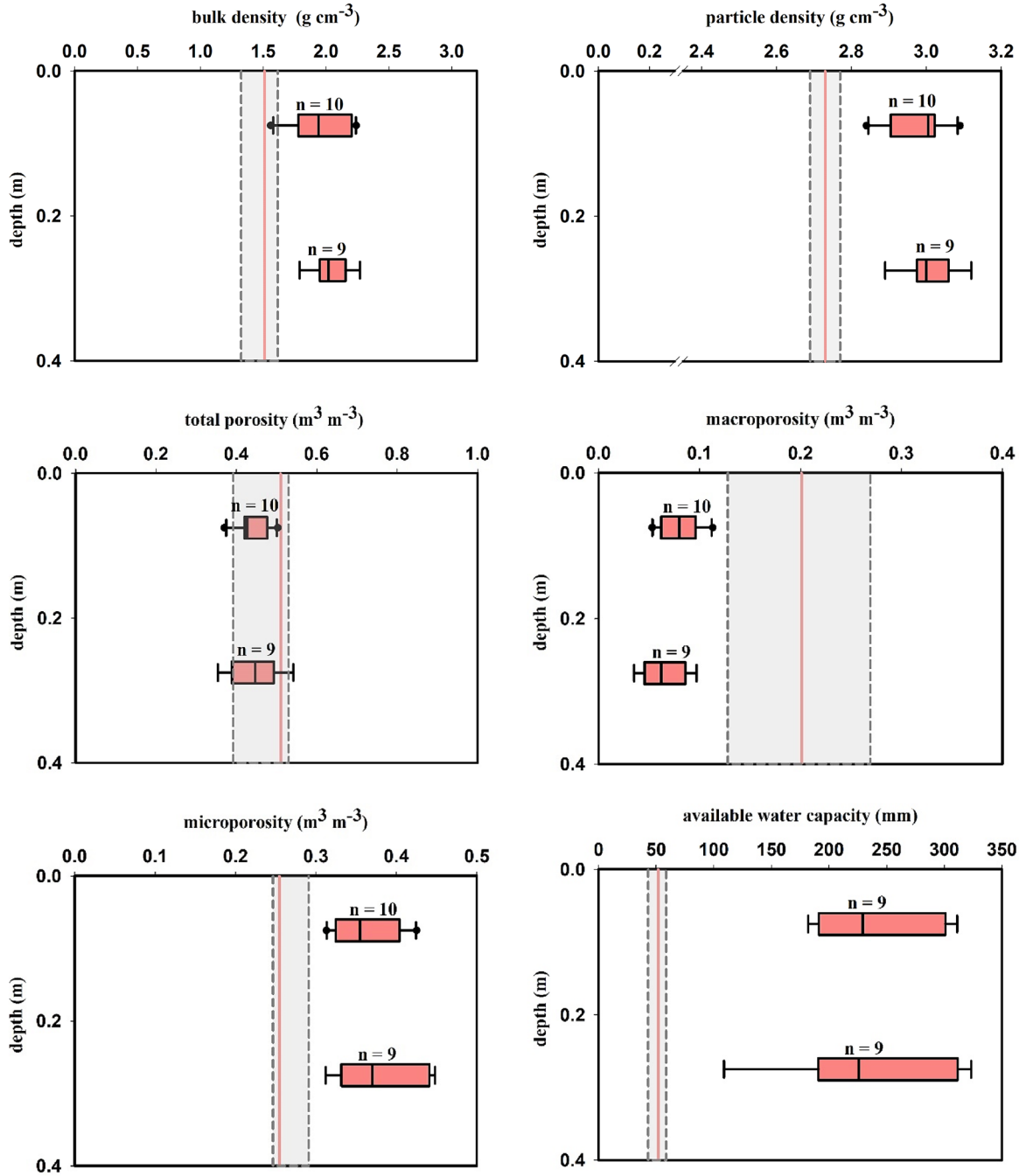

Fig. 6 Physical parameters of the Technosols (deposited iron tailings (DIT)) collected from 10 cross-sections in the Doce River basin. Vertical lines separated by hatched areas represent the limits of the first and third quartiles of the baseline, and the red vertical line represents the median of the baseline from Ottoni et al. (2018), except for particle density, which is from Pacheco (2015)

attributed to the enrichment of DIT by iron oxides (Fig. 4), which contributes to a higher particle density compared with the more silicate-rich baseline soils (Pacheco, 2015; Rodrigues, 2012). Silicate minerals, such as quartz, typically exhibit an average particle density of approximately 2.65 g cm^{-3}, and the particle density of iron oxides approaches 3.0 g cm^{-3} (Fig. 6). This discrepancy in particle density between silicate minerals and iron oxides contributes to the overall increase in particle density observed in the DIT. Additionally, the reduced organic carbon content in the DIT (Fig. 5) further contributes to the elevated Dp of tailings.

The high bulk density (Db) observed in the DIT, exceeding the recommended thresholds for both clayey and loamy/sandy soils (> 1.3 g cm^{-3} and > 1.6 g cm^{-3}, respectively), coupled with the low total porosity (TP), particularly characterized by reduced macroporosity (Ma), imposes significant constraints on soil drainage and root growth of plants (Reichert et al., 2000).

The reduction in Ma of the DIT compared with the baseline soils (Fig. 6) is of particular concern as the median macroporosity (Mi) of the DIT has remained at 7% across the 0–0.4 m layer, falling below the minimum threshold of 10% to avoid restrictions in for root development (Baver et al., 1972). This decline in Mi directly corresponds to the absence of soil structure, notably aggregation, within the DIT. During the process of tailing dragging, loose particles of sand, silt, and clay settle hierarchically based on their size, resulting in a compacted soil matrix and subsequently reduced Ma (Brady & Weil, 2002; Hillel, 1998).

The reduction in Ma in the DIT has not yielded a significant difference in TP, as it was counterbalanced by an increase in Mi (Fig. 6). Micropores, characterized by diameters less than 0.05 mm, predominantly form between mineral and organic particles and play a crucial role in storing water essential for plant uptake (Reichert et al., 2003).

The increase in water availability in the DIT can be attributed to differences in texture between pre- and post-disaster matrices. The increase in the silt fraction, characterized by its larger specific surface area, contrasts with the predominance of the sand fraction observed in the alluvial soils adopted as baseline (Fig. 3), resulting in a heightened water retention potential, primarily attributable to the matrix component of the soil (O'Geen, 2013). However, compaction and reduction of macropores in the DIT may restrict root development and increase the occurrence of erosive processes, especially in areas devoid of vegetation cover.

Technosol chemical fertility

The median value of pH in water (pH_{H2O}) has not varied with depth (Fig. 7). In both the upper and lower layers of DIT, the median pH_{H2O} values (6.2 and 6.0, respectively) have surpassed those of the baseline. The mineral ore (Itabirito) processing undergoes milling, desliming, and flotation, with the final loading stage employing NaOH and ether monoamine ($pH_{H2O} = 10.5$) (Vasconcelos et al., 2012). Some DIT samples have pH_{H2O} values exceeding 7.0, with a maximum reaching 8.5 (Fig. 7). Another determining factor for the high pH_{H2O} in DIT is the presence of excessive water in the mining containment dams and floodplains along the margins of the Doce River (Melo et al., 2023). Additionally, under reducing conditions characterized by low redox potential, the pH of the tailings stabilizes at values near neutral (Queiroz et al., 2018) due to the inverse relationship between redox potential (pe) and pH, where higher electron activity corresponds to lower proton activity in the environment (Lindsay, 1979).

Another distinct characteristic of DIT was the prevalence of positive charges (AEC) over the negative charges (CEC): positive delta pH ($pH_{KCl} > pH_{H2O}$) observed at both depths (Fig. 7). In contrast, baseline soils exhibit electronegativity ($pH_{KCl} < pH_{H2O}$). The predominance of positive charge is uncommon in soils, especially in the A horizon, occurring in B horizons of highly weathered soils in humid tropical regions (Acric Oxisols). Consistent with previous findings (Santos et al., 2019), the predominance of AEC in the DIT is reflected in its lower CEC compared with the baseline soils (Fig. 7). This is consistent with the higher point of zero charge (ZPC) in the DIT (between 6 and 7) (Almeida et al., 2018; Grilo et al., 2020), as there was a combination of low organic matter content and the prevalence of Fe oxides in their clay fraction (Fig. 4 and Fig. 5).

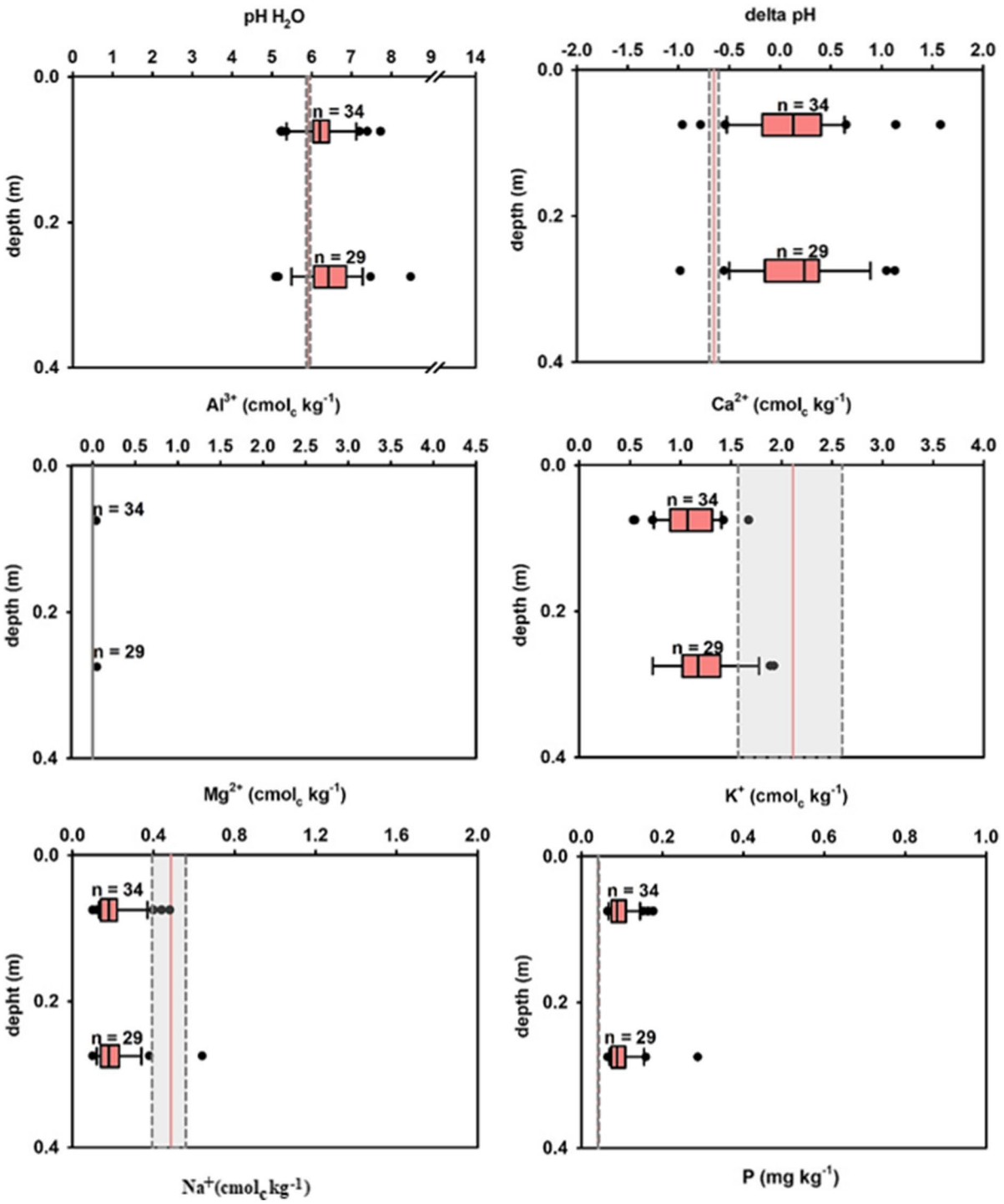

Fig. 7 Chemical fertility of the Technosols (deposited iron tailings (DIT)) collected in 10 transverse sections in the Rio Doce basin. Vertical lines separated by hatched areas represent the limits of the first and third quartiles of the baseline, and the red vertical line represents the baseline median (Pacheco, 2015)

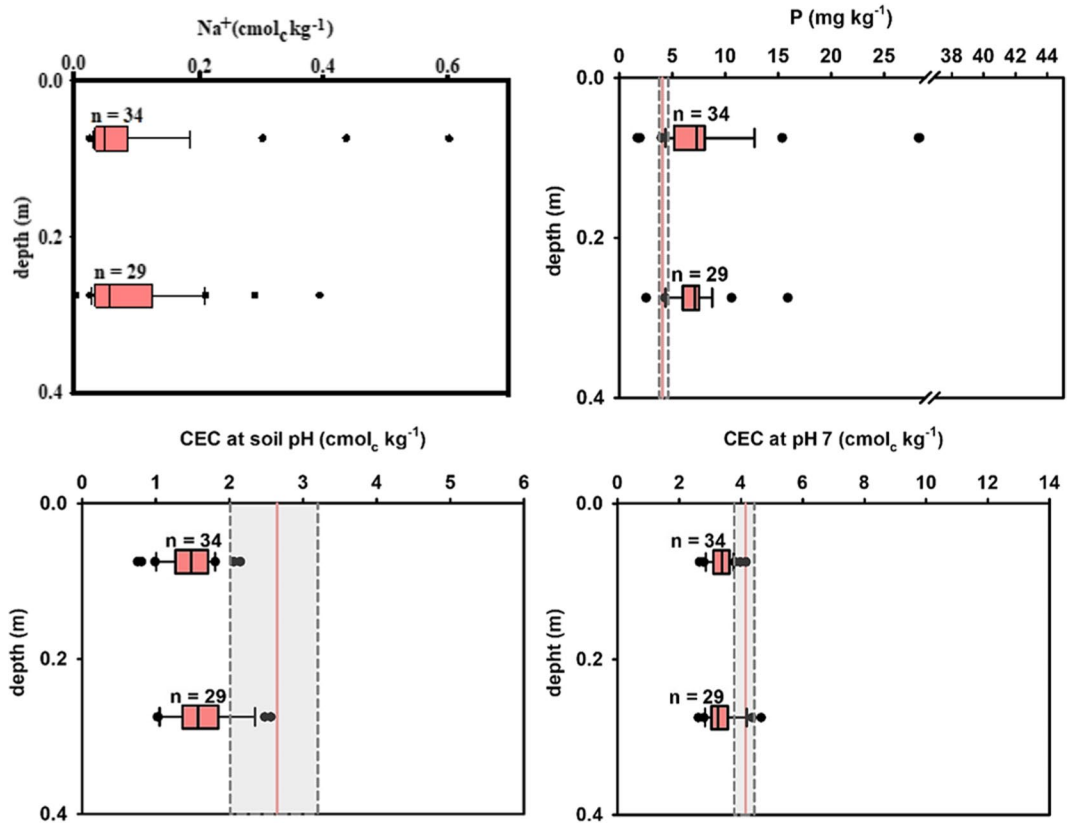

Fig. 7 (continued)

Iron oxides present low CEC compared with kaolinite, which has a ZPC around 3.5 (Tarì et al., 1999). The low pka of the silanol group at the edges of tetrahedral sheet determines the reduction of the kaolinite's ZPC: (i) pH < 2.0, the silanol group is protonated (—Si–OH), and there is no formation of charges; (ii) pH > 2.0, there is deprotonation of the silanol group (—Si–O^-) and formation of negative charges (CEC). The ZPC of Fe oxides (Hm and Gt) is higher and lies above the neutrality, ranging between 8 and 9 (Schwertmann & Taylor, 1989): (i) pH < ZPC (highest occurrence of —Fe-$OH_2^{+0.5}$ group, followed by the monoprotonated species —Fe-$OH^{-0.5}$), predominance of positive charges (AEC > CEC); (ii) pH > ZPC (highest occurrence of —Fe-$OH^{-0.5}$ group, followed by the deprotonated species —$FeO^{-1.5}$), predominance of negative charges (CEC > AEC). Given that the pH_{H2O} of DIT falls between the ZPC values of kaolinite and iron oxides, a scenario arises where CEC predominates in kaolinite, while AEC prevails in hematite and goethite. To enhance the negative charges in DIT, the most recommended practice involves increasing organic matter content, as organic compounds have a ZPC below 4.0 (Schmitt et al., 2018). The main adsorption sites that deprotonate and form negative charges in organic matter are carboxyl (-COOH), alcoholic hydroxyl (-OH), and phenolic hydroxyl (-OH) (Lin et al., 2017). The carboxyl group of the organic matter is more important and deprotonates at pH greater than 4.0 and form negative charges (CEC) (Schmitt et al., 2018).

The absence of exchangeable Al in the tailings (Fig. 7) can be attributed to pH_{H2O} higher than 5.5 (Lindsay, 1979). At pH_{H2O} of 6.0–6.2 of the DIT, almost 100% of soil Al will be in the nontoxic $Al(OH)_3^0$ form. The reduced exchangeable Ca concentrations in the 0–0.2 m layer of DIT (1.1 $cmol_c$ kg^{-1}) were lower than the baseline value of 2.1 $cmol_c$ kg^{-1} (Fig. 7), and this trend is mirrored for

exchangeable Mg. Calcium shortage are an important factor to liming the plant growth.

On the other hand, the median available K concentration in DIT (0.09 $cmol_c\ kg^{-1}$) has surpassed the baseline value of 0.04 $cmol_c\ kg^{-1}$ (Fig. 7). There was also an enrichment in P content with the tailing deposition (Fig. 7). Chemical products containing P have been employed in the process of residue dispersion, such as sodium polyphosphate (Vasconcelos et al., 2012). Other authors have observed similar patterns in the chemical fertility of Technosols affected by the disaster along the Doce River margins (Santos et al., 2019).

Plant (*Urochloa* sp.) nutritional composition

The contents of Ca, K, and P in *Urochloa* sp. were slightly higher and similar for Mg in plants grown on CS than on DIT (Fig. 8), suggesting that tailing deposition has not compromised the nutritional composition of plants. Cruz et al. (2020) have compared nutrient concentrations in five species of tree seedlings growing on tailings and on the natural soil along the Doce River floodplains and observed higher Ca contents in all species and higher P contents in three species on tailings?

Dairy farming is the main economic activity in the study region, and the analysis of nutrient composition in *Urochloa* sp. collected from various positions along DIT, STM, and CS transects has revealed a concerning inadequacy in meeting the nutritional requirements for such activity, particularly Ca, K, and P. According to the recommendations outlined by NRC (2001), lactating cows require concentrations of 5300 mg kg^{-1} for Ca, 10,000 mg kg^{-1} for K, and 4400 mg kg^{-1} for P in their diet. Therefore, the exclusive consumption of *Urochloa* sp. from all transect positions falls short of meeting these requirements. However, it is important to highlight that less than 2% of Brazilian pastures are regularly fertilized (Anda, 2022).

The initial remediation strategy for soils affected by Fe tailings would be the application of mineral and organic fertilizers. However, fertilization may not represent proportional gains in plant quality due to the high contents of Fe and Mn in the tailings (Melo et al., 2023). Although fertilization can provide adequate levels of plant nutrients such as N, P,

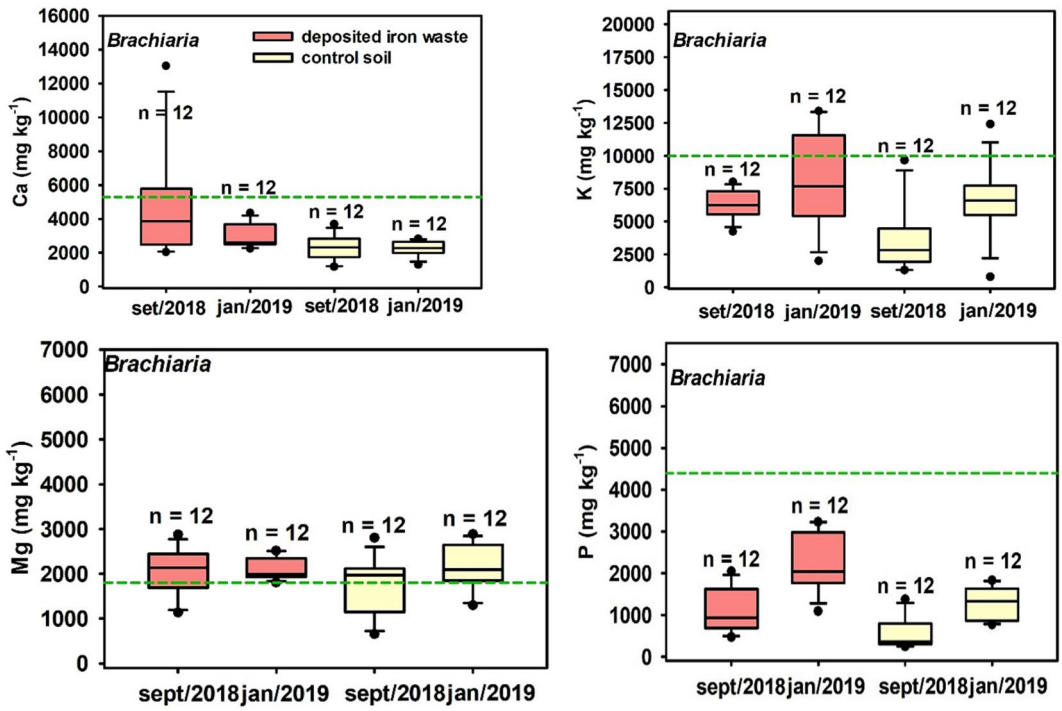

Fig. 8 Macronutrient concentrations in shoot tissue of *Urochloa* sp. (*Brachiaria*) grown on deposited iron tailings (DIT) and control soils (CS). The green horizontal line represents the minimum nutrient requirement for lactating dairy cows (NRC, 2001)

K, Ca, and Mg, it has not fully mitigated the negative effects of iron tailings on plant tissues. High concentrations of Fe in plant tissues have been associated with decreased biomass production, stunted growth, reduced leaf area, altered leaf morphology, and diminished chlorophyll content. These observations suggest a potential phytotoxic effect of the elevated Fe levels present in the DIT (Cruz et al., 2022).

Conclusions and recommendations

The replacement of the pre-disaster kaolinitic matrix by post-disaster hematitic mineralogy, coupled with the reduction in organic carbon content and the prevalence of silt particles in the deposited iron tailings (DIT), was the most severe detected effects on floodplains, which has triggered various detrimental consequences, such as the reduction in DIT's cation exchange capacity (CEC). Highly complex organic matter management is necessary for mitigating CEC reduction and compensating for the hematitic matrix prevalence.

The physical deterioration in the DIT (Technosol), characterized by increased bulk density and reduced macroporosity and total porosity, favors erosive processes in the Technosol. Organic matter input plays a crucial mitigating role by promoting particle flocculation and soil aggregation, a fundamental step toward Technosol physical rehabilitation.

Melo et al. (2023) and others researches on the Doce River basin have not observed contamination with potentially toxic metals and non-metals in the affected area. In contrast, the present study has revealed significant damage and loss of environmental quality associated with physical, chemical, and mineralogical alterations in the DIT. Given these findings, it is essential to reassess the priorities of future research in the disaster-affected region to better support rehabilitation practices.

Acknowledgements This work is a part of the Socioenvironmental Diagnosis of the Damages Arising from the Fundão Dam Rupture in the Doce River basin. Technical materials are accessible at http://www.mpf.mp.br/grandes-casos/caso-samarco/atuacaodo-mpf/pareceres-e-relatorios/instituto-lactec. The authors express gratitude to the Instituto de Tecnologia para o Desenvolvimento (LACTEC) for its support and also thank the Federal Prosecution Service (Ministério Público Federal—MPF), the State Prosecution Services of Minas Gerais and Espirito Santo (Ministério Público do Estado de Minas Gerais—MPMG), and the Ministério Público do Estado do Espirito Santo—MPES) for the opportunity to contribute to Samarco's Fundão Dam Rupture case.

Author contribution A.C.V. Motta, L.de Pierri, B. Lipski, V.F. Melo, T.M. Ercole, M.F.D.S. Lima, L.P. Bastos, R.S. Corrêa had balanced involvement in all the following items and steps for the idealization and preparation of the manuscript: Conceptualization, Data curation, Formal analysis, Funding acquisition (not applicable), Investigation, Methodology, Project administration, Software, Supervision, Validation, Visualization, Writing – original draft and Writing – review & editing.

Data availability No datasets were generated or analysed during the current study.

Declarations

Consent for publication All authors have approved the manuscript and agree with its publication to *Environmental Monitoring and Assessment*.

Competing interests The authors declare no competing interests.

References

Almeida, C. A., Oliveira, A. F., Pacheco, A. A., Lopes, R. P., Neves, A. A., & Queiroz, M. E. L. R. (2018). Characterization and evaluation of sorption potential of the iron mine tailing after Samarco dam disaster in Doce River basin - Brazil. *Chemosphere, 209*, 411–420. https://doi.org/10.1016/j.chemosphere.2018.06.071

ANDA. (2022). *Fertilizer Sector – Statistical Yearbook*. National Association for the Diffusion of Fertilizers (NADF)

Azam, S., & Li, O. (2010). Tailings dam failures: A review of the last one hundred years. Geotechnical News, 50–53. https://doi.org/10.1016/j.gloenvcha.2021.102361

Baver, L. D., Gardner, W. H., & Gardner, W. R. (1972). *Soil physics* (4th ed.). John Wiley & Sons Inc.

Brady, N. C., & Weil, R. R. (2002). *The nature and properties of soils* (13th ed.). Prentice Hall.

Carmo, F. F., Kamino, L. H. Y., Junior, R. T., Campos, I. C., Carmo, F. F., Silvino, G., & Pinto, C. E. F. (2017). Fundão tailings dam failures: The environment tragedy of the largest technological disaster of Brazilian mining in global context. *Perspectives in Ecology and Conservation, 15*, 145–151. https://doi.org/10.1016/j.pecon.2017.06.002

Coelho, D. G., Marinato, C. S., Matos, L. P., Andrade, H. M., Silva, V. M., Neves, P. H. S., & Oliveira, J. A. (2020). Evaluation of metals in soil and tissues of economic-interest plants grown in sites affected by the Fundão dam failure in Mariana, Brazil. *Integrated Environmental*

Assessment and Management, 16, 596–607. https://doi.org/10.1002/ieam.4253

Cruz, F. V. S., Gomes, M. P., Bicalho, E. M., & Garcia, Q. S. (2022). Fertilization assures mineral nutrition but does not overcome the effects of Fe accumulation in plants grown in iron ore tailings. *Environmental Science and Pollution Research, 29*, 18047–18062. https://doi.org/10.1007/s11356-021-16989-3

Cruz, F. V. S., Gomes, M. P., Bicalho, E. M., Torre, F. D., & Garcia, Q. S. (2020). Does Samarco's spilled mud impair the growth of native trees of the Atlantic Rainforest? *Ecotoxicology and Environmental Safety, 189*, 1–12. https://doi.org/10.1016/j.ecoenv.2019.110021

Davila, R. B., Fontes, M. P. F., Pacheco, A. A., & Ferreira, M. S. (2020). Heavy metals in iron tailings and floodplain soils affected by the Samarco dam collapse in Brazil. *Science of the Total Environment, 709*, 1–11. https://doi.org/10.1016/j.scitotenv.2019.136151

Duarte, E. B., Neves, M. A., Oliveira, F. B., Martins, M. E., Oliveira, C. H. R., Burak, D. L., Orlando, M. T. D., & Rangel, C. V. G. T. (2021). Trace metals in Rio Doce sediments before and after the collapse of the Fundão iron ore tailing dam, Southeastern Brazil. *Chemosphere, 262*, 1–9. https://doi.org/10.1016/j.chemosphere.2020.127879

Embrapa. (2017). *Manual of Soil Analysis Methods* (3rd ed.). Centro Nacional de Pesquisa de Solos, Embrapa.

Gabriel, F. A., Silva, A. G., Queiroz, H. M., Ferreira, T. O., Hauser-Davis, R. A., & Bernardino, A. F. (2020). Ecological risks of metal and metalloid contamination in the Rio Doce Estuary. *Integrated Environmental Assessment and Management, 16*, 655–660. https://doi.org/10.1002/ieam.4250

Gamie, R., & Smedt, F. (2017). Experimental and statistical study of saturated hydraulic conductivity and relations with other soil properties of a desert soil. *European Journal of Soil Science, 69*, 256–264. https://doi.org/10.1111/ejss.12519

Grilo, C. F., Chassagne, C., Quaresma, V. S., Kan, P. J. M., & Bastos, A. C. (2020). The role of charge reversal of iron ore tailing sludge on the flocculation tendency of sediments in marine environment. *Applied Geochemistry, 117*, 1–10. https://doi.org/10.1016/j.apgeochem.2020.104606

Hatje, V., Pedreira, R. M. A., Rezende, C. E., Schettini, C. A. F., Souza, G. C., Marin, D. C., & Hackspacher, P. C. (2017). The environmental impacts of one of the largest tailings dam failures worldwide. *Scientific Reports, 7*, 1–13. https://doi.org/10.1038/s41598-017-11143-x

Hillel, D. (1998). *Environmental soil physics* (1st ed.). Academic Press.

Islam, K., & Murakami, S. (2021). Global-scale impact analysis of mine tailings dam failures: 1915–2020. *Global Environmental Change, 70*, 102361.

Lin, J., Zhang, Z., & Zhan, Y. (2017). Effect of humic acid preloading on phosphate adsorption onto zirconium-modified zeolite. *Environmental Science and Pollution Research, 24*, 12195–12211.

Lin, S.-Q., Wang, G.-J., Liu, W.-L., Zhao, B., Shen, Y.-M., Wang, M.-L., & Li, X.-J. (2022). Regional distribution and causes of global mine tailings dam failures. *Metals, 12*, 905. https://doi.org/10.3390/met12060905

Lindsay, W. L. (1979). *Chemical equilibria in soils* (1st ed.). John Wiley and Sons.

Mello, D. C., Dematte, J. A. M., Silvero, N. E. Q., Di Raimo, L. A. D., Fellipe, R. R. P., Mello, A. O., Souza, A. B., Safanelli, J. L., Resende, M. E. B., Rizzo, R. (2020). Soil magnetic susceptibility and its relationship with naturally occurring processes and soil attributes in pedosphere, in a tropical environment. Geoderma, 114364. https://doi.org/10.1016/j.geoderma.2020.114364

Melo, V. F., Lipski, B., Motta, A. C. V., Pierri, L., Leme, D. M., Ercole, T. M., Lima, M. F. D. S., Thá, E. L., & Bastos, L. P. (2023). Integrated environmental assessment of iron ore tailings in floodplain soils and plants after the Fundão Dam disaster in Brazil. *Integrated Environmental Assessment and Management, 20*, 117–132. https://doi.org/10.1002/ieam.4780

Munsell soil color company. (1950). *Munsell soil color chats: Munsell color*. Macbeth Division of Kollmorgen Coporation.

NRC. (2001). *Nutrient requirements of dairy cattle* (7th. ed.). The National Academies Press.

Nungesser, S. R., & Pauliuk, S. (2022). Modelling hazard for tailings dam failures at copper mines in global supply chains. *Resources, 11*, 95. https://doi.org/10.3390/resources11100095

O'Geen, A. T. (2013). Soil Water Dynamics. *Nature Education Knowledge, 4*, 1–9.

Orlando, M. T. D., Galvão, E. S., Cavichini, A. S., Rangel, C. V. G. T., Orlando, C. G. P., Grilo, C. F., Soares, J., Oliveira, K. S. S., Sá, F., Junior, A. C., Bastos, A. C., & Quaresma, V. S. (2020). Tracing iron tailings in the marine environment: An investigation of the Fundão Dam failure. *Chemosphere, 257*, 1–9. https://doi.org/10.1016/j.chemosphere.2020.127184

Ottoni, M. V., Ottoni Filho, T. B., Schaap, M. G., Lopes-Assad, M. L. R. C., & Rotunno Filho, O. C. (2018). Hydrophysical database for Brazilian soils (HYBRAS) and pedotransfer functions for water retention. *Vadose Zone Journal, 17*, 1–17. https://doi.org/10.2136/vzj2017.05.0095

Pacheco, A. A. (2015). Assessment of contamination in soils and sediments of the Doce river basin by heavy metals and their relationship with the natural geochemical background [Doctoral dissertation, Universidade Federal de Viçosa]. Universidade Federal de Viçosa Digital Repository. https://www.locus.ufv.br/handle/123456789/6465. Accessed Dec 2015

Pulley, S., Collins, A. L., & Van der Waal, B. (2018). Variability in the mineral magnetic properties of soils and sediments within a single field in the Cape Fold mountains, South Africa: Implications for sediment source tracing. *CATENA, 163*, 172–183. https://doi.org/10.1016/j.catena.2017.12.019

Queiroz, H. M., Nóbrega, G. N., Ferreira, T. O., Almeida, L. S., Romero, T. B., Santaella, S. T., Bernardino, A. F., & Otero, X. L. (2018). The Samarco mine tailing disaster: A possible time-bomb for heavy metals contamination. *Science of the Total Environment, 637–638*, 498–506. https://doi.org/10.1016/j.scitotenv.2018.04.370

Ramos, M. R., Melo, V. F., Uhlmann, A., Dedecek, R. A., & Curcio, G. R. (2015). Clay mineralogy and genesis of fragipan in soils from Southeast Brazil. *CATENA, 135*, 22–28. https://doi.org/10.1016/j.catena.2015.06.016

Reichert, J. M., Reinert, D. J., & Braida, J. A. (2003). Soil quality and sustainability of agricultural systems. *Ciência e Ambiente, 27*, 29–48.

Rico, M., Benito, G., Salgueiro, A. R., Dıez-Herrero, A., & Pereira, H. G. (2008). Reported tailings dam failures: A review of the European incidents in the worldwide context. *Journal of Hazardous Materials, 152*, 846–852. https://doi.org/10.1016/j.jhazmat.2007.07.050

Rodrigues, A. S. D. L. (2012). Characterization of the Gualaxo do Norte River basin, MG, Brazil: Environmental geochemical assessment and proposition of background values [Doctoral dissertation, Universidade Federal de Ouro Preto]. Universidade Federal de Ouro Preto Digital Repository. https://www.repositorio.ufop.br/handle/123456789/4139. Accessed Dec 2015

Rossiter, D. G. (2007). Classification of urban and industrial soils in the world reference base for soil resources. *Journal of Soils and Sediments, 7*, 96–100. https://doi.org/10.1065/jss2007.02.208

Santos, O. S. H., Avellar, F. C., Alves, M., Trindade, R. C., Menezes, M. B., Ferreira, M. C., França, G. S., Cordeiro, J., Sobreira, F. G., Yoshida, I. M., Moura, P. M., Baptista, M. B., & Scotti, M. R. (2019). Understanding the environmental impact of a mine dam rupture in Brazil: Prospects for remediation. *Journal of Environmental Quality, 48*, 439–449. https://doi.org/10.2134/jeq.2018.04.0168

Schmitt, D. E., Gatiboni, L. C., Orsoletta, D. J. D., & Brunetto, G. (2018). Formation of ternary organic acids-Fe-P complexes on the growth of wheat (Triticum aestivum). *Revista Brasileira De Engenharia Agrícola e Ambiental, 22*, 702–706.

Schwertmann, U., & Taylor, R. M. (1989). Iron oxides. In J. B. Dixon & S. B. Weed (Eds.), *Minerals in soil environments* (2nd ed., pp. 379–438). Soil Science Society of America.

Silva, A. O., Guimarães, A. A., Lopez, B. D. O., Zanchi, C. S., Vega, C. F. P., Batista, E. R., Moreira, F. M. S., Souza, F. R. C., Pinto, F. A., Santos, J. V., Carneiro, J. J., Siqueira, J. O., Kemmelmeier, K., Guilherme, L. R. G., Rufini, M., Dias Junior, M. S., Aragão, O. O. S., Borges, P. H. C., Oliveira-Longatti, S. M., & Carneiro, M. A. C. (2021). Chemical, physical, and biological attributes in soils affected by deposition of iron ore tailings from the Fundão Dam failure. *Environmental Monitoring and Assessment, 193*, 1–18. https://doi.org/10.1007/s10661-021-09234-4

Tarì, G., Bobos, I. I., Gomes, C. S. F., & Ferreira, J. M. F. (1999). Modification of surface charge properties during kaolinite to halloysite-7Å transformation. *Journal of Colloid and Interface Science, 210*, 360–366. https://doi.org/10.1006/jcis.1998.5917

Vasconcelos, J. A., Brandão, P. R. G., & Lemos, L. N. (2012). Characterization and concentration studies of compact itabirite from the Serra Azul Complex, MG. *Tecnologica Em Metalurgia, Materiais e Mineração, 9*, 89–94. https://doi.org/10.4322/tmm.2012.014